2021 20th IEEE Intersociety Conference on Thermal and Thermomechanical Phenomena in Electronic Systems (iTherm) | 978-1-7281-8539-2/21/$31.00 ©2021 IEEE | DOI: 10.1109/ITherm51669.2021.9503186

Two-Dimensional Actuation of Liquid-Metal Droplets for Hot-Spot Cooling

Saige J. Dacuycuy
Department of Electrical Engineering
University of Hawai'i
Honolulu, HI, USA
saiged@hawaii.edu

Wayne A. Shiroma
Department of Electrical Engineering
University of Hawai'i
Honolulu, HI, USA
shiromaw@hawaii.edu

Aaron T. Ohta
Department of Electrical Engineering
University of Hawai'i
Honolulu, HI, USA
aohta@hawaii.edu

***Abstract*— A liquid-metal droplet is actuated in a two-dimensional plane to demonstrate controlled actuation and selective hot-spot cooling. Continuous electrowetting actuates the droplet to move along a prescribed path within a 3 cm ✖ 3 cm well. The terminal velocity of the actuated droplet is achieved at 13.3 cm/s with an actuation voltage of 11 V DC. Increasing the number of electrodes along the well edges results in more precise positioning of the liquid-metal droplet. This technique allows an actuated droplet to perform rapid cooling at localized hot spots within the device. For an actuation voltage of 10 V DC, the liquid-metal droplet decreases the temperature of a hot spot by approximately 7 °C.**

Keywords*— *continuous electrowetting, liquid metal, thermal management

I. Introduction

The deformable nature and electrical conductivity of liquid metals make them useful in areas such as sensors, microfluidic components, flexible electronics, and reconfigurable devices [1]–[4]. When an external electric potential gradient is applied to liquid metal residing in an electrolytic solution, locomotive properties can also be realized [5], [6], making them useful for performing physical tasks when equipped with microtools [7]. Due to their precise positioning capability under low external electrical fields, liquid-metal droplets have recently shown promise for electronic thermal management, particularly in light of increasing integrated-circuit densities that are stretching the limits of Moore's Law [8].

This paper presents a hot-spot cooling technique in which a liquid-metal droplet is actuated toward an arbitrarily located hot spot, then actuated away from that hot spot to facilitate rapid cooling. Actuation is achieved via continuous electrowetting (CEW) [9], in which a voltage is applied to a non-toxic, room-temperature, liquid-metal alloy Galinstan droplet residing in a solution of sodium hydroxide (NaOH) [10]. The droplet moves along arbitrarily prescribed trajectories in an open two-dimensional plane, with electrodes embedded in the walls of a polydimethylsiloxane (PDMS) well.

The only known previous work using a CEW-based liquid-metal droplet cooling system is [11], in which the droplet transports heat away from a hot spot within a closed-loop channel; however, this limits the hot spot to a fixed location along that closed loop. In our work, the locations of the hot spot and heat sink are both arbitrarily located within a two-dimensional plane, making this paper the first investigation combining the electrical actuation of a liquid-metal droplet along arbitrarily prescribed trajectories for selective hot-spot cooling.

II. Two-Dimensional Actuation

A. Experimental Setup

To demonstrate the actuation of liquid-metal droplets in 2D, a well with integrated electrodes was fabricated (Fig. 1). A 3 cm × 3 cm × 0.8 cm well was cut into a layer of PDMS that was bonded on a flat piece of polystyrene. The well is filled with 1 M NaOH and contains a Galinstan liquid-metal droplet with a volume of approximately 0.07 ml. Nickel strips serve as the electrodes of the well and are embedded into the PDMS walls by transfixing nickel rods into the electrodes and the PDMS. Voltages applied to these electrodes are used for CEW actuation. The applied voltages create surface-tension gradients and Marangoni forces at and near the surface of the liquid-metal droplet, causing it to move. Thus, to actuate the liquid-metal droplet, a voltage is applied to a single electrode while grounding the other electrodes. The droplet moves toward the higher-voltage electrode. To reverse the direction of motion, the voltage polarity on the electrodes is switched.

Two identical wells were constructed with different electrode placements. The 4-electrode well used four nickel strips as the electrodes, each 2.8 cm long. The 12-electrode well used 12 nickel strips, each 0.7 cm long.

An Arduino Mega ADK was used to control the electrode voltages. For the 4-electrode well, one STMicroelectronics L298N dual H-bridge motor driver was used to move the droplet in cardinal directions. For the 12-electrode well, three L298N motor drivers were used to move the droplet in both cardinal and intercardinal directions.

A Sony HDR-CX580V camera mounted on a tripod recorded the movement of the droplet. The droplet velocity from electrode to electrode was determined with an open-source software, *Tracker*, by measuring the position of the droplet between the video frame rates [12].

B. Results and Discussion

Fig. 2 shows the actuation of the droplet in a 4-electrode well and 12-electrode well. In both cases, the droplet moved from the left electrode to the right electrode in a straight path.

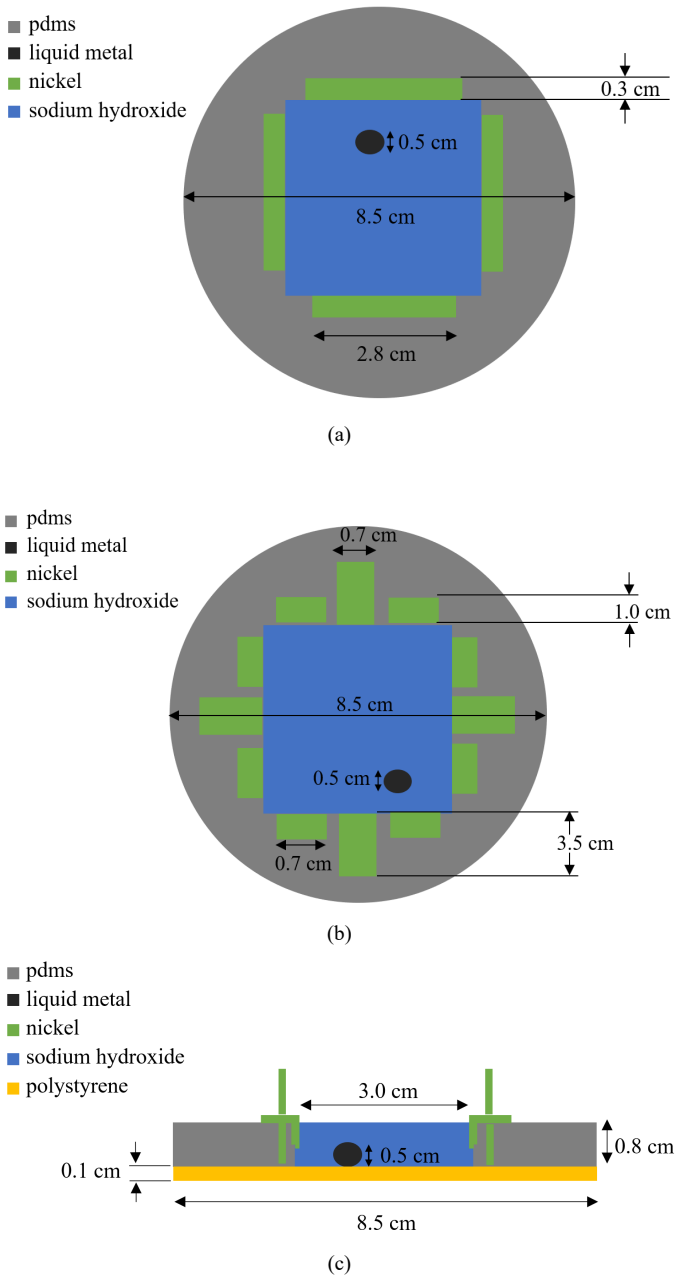

Fig. 1. Layout of actuation device: (a) top view of 4-electrode device; (b) top view of 12-electrode device; (c) cross-sectional view of device well.

Fig. 3 shows the droplet's maximum velocity as a function of voltage. The droplets reached a 13.3-cm/s terminal velocity at approximately 11 V DC, suggesting that the actuation process for the device does not require an actuation voltage greater than 11 V DC.

In addition to the droplet moving in a straight path, as shown in Fig. 2, the droplet can move along an arbitrary path (Fig. 4). To achieve this, a potential of 11 V was first applied to Electrode 2 while Electrode 1 was grounded. After the droplet moved to the desired position near Electrode 2, Electrodes 1 and 2 were grounded, and 11 V was applied to Electrode 3. It was only possible to move the droplet along a path like this using the 12-electrode well, so increasing the number of electrodes increases

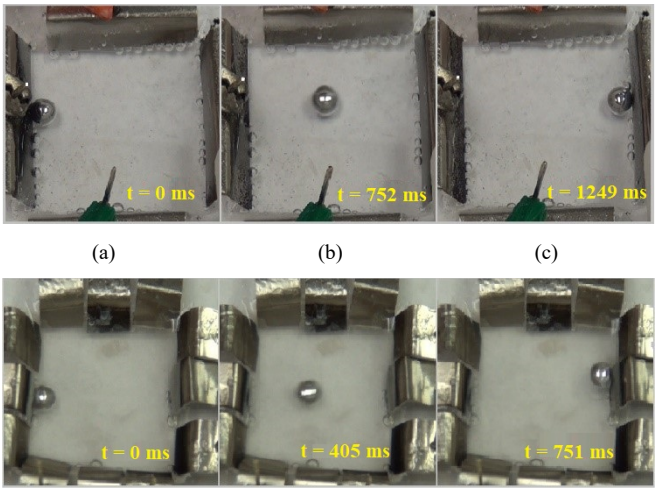

Fig. 2. Actuation of the liquid-metal droplet along a straight-line path for the (a)–(c) 4-electrode and (d)–(f) 12-electrode well. From left to right: starting electrode, middle of the well, and opposite electrode. In all cases, the actuation voltage is 7.5 V DC.

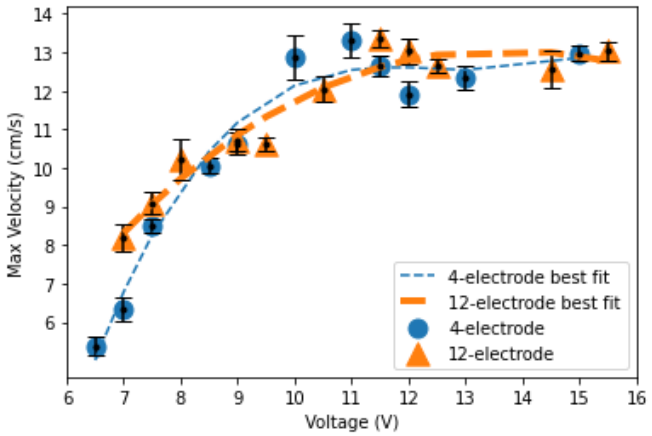

Fig. 3. Droplet velocity as a function of voltage.

the precision of motion of the droplet. Applying voltages sequentially can change the droplet's trajectory. By selectively choosing which electrodes to attract the droplet, more complex paths can be realized.

III. Hot-Spot Cooling

A. Experimental Setup

For this experiment, the 12-electrode well configuration was modified by using stainless steel electrodes and merging the top-right electrodes and the bottom-left electrodes (Fig. 5). The enlarged electrode geometry covers opposite corners of the PDMS well, and serves multiple purposes. The top-right electrode is used to generate a localized hot spot, and the bottom-left electrode serves as a rudimentary heat sink. At the same time, the top-right and bottom-left electrodes can still be used for CEW actuation. The larger area of the top-right and bottom-left electrodes help with imaging of the temperature in the system using an infrared camera; however, it is possible to achieve similar results with the original 12-electrode configuration as well.

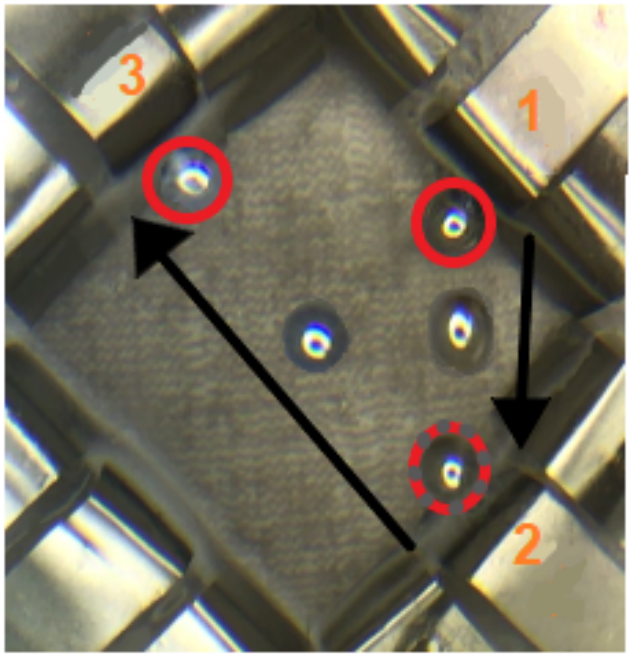

Fig. 4. Actuation of the liquid-metal droplet along an arbitrary path. The desired path is indicated by the black arrows and the droplets outlined in red are the initial and final positions of the traveling droplet. The red dashed circle is the position of the droplet midway through the actuation sequence. The potential difference between the actuating electrode pairs was 11 V. The electrodes used in this actuation sequence are numbered for reference.

To demonstrate the concept of Fig. 5, a hot spot is created then cooled once the liquid-metal droplet is injected and actuated to the hot spot (Fig. 6). The well is first filled with 1-M NaOH, and a positive voltage is then applied to the top-right electrode for a period of 165 s. During this period, the applied voltage heats up the NaOH, creating a hot spot near the top-right electrode [Fig. 6(a)]. After 150 s of electrode activation, a liquid-metal droplet is manually injected by a syringe into the middle of the well. The droplet moves toward the top-right electrode via CEW within 1 second, and cools the hot spot [Fig 6(b)–(c)]. The droplet occupies the hot spot for approximately 10 s, then the polarity is switched between the top-right electrode and the bottom-left electrode, and the droplet moves in the direction of the bottom-left electrode, which serves as a rudimentary heat sink. The droplet takes approximately 1 second to move from the top right to the bottom left, and is kept in contact with the heat sink for the remainder of the experiment [Fig. 6(d)].

B. Thermal Effects of Applied Voltages

An experiment was conducted to measure the Joule heating of the NaOH caused by the CEW actuation voltages. To isolate this effect, no liquid metal was in the PDMS well. The temperature was measured at the top-right corner of the well when a voltage of 10 V or 11 V was applied to the top-right electrode while the other electrodes were grounded (Fig. 7). For the 2D actuation discussed in Section II.B, the CEW voltages are applied for less than 1 s; thus, to quantify the Joule heating, the temperature was measured for a period of 10 s [Fig. 7(b)] to show that the applied voltage does not cause any appreciable heating in the actuation time window.

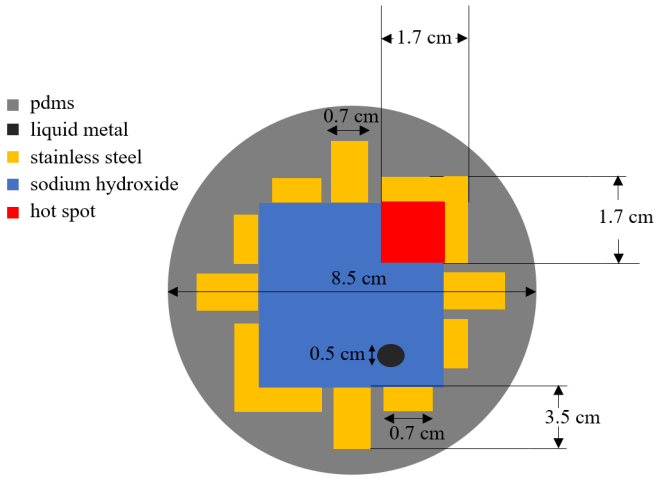

Fig. 5. Layout of 10-electrode device. The red region in the well is the hot spot generated by applying a voltage to the top-right electrode, which in turn heats up a section of the NaOH.

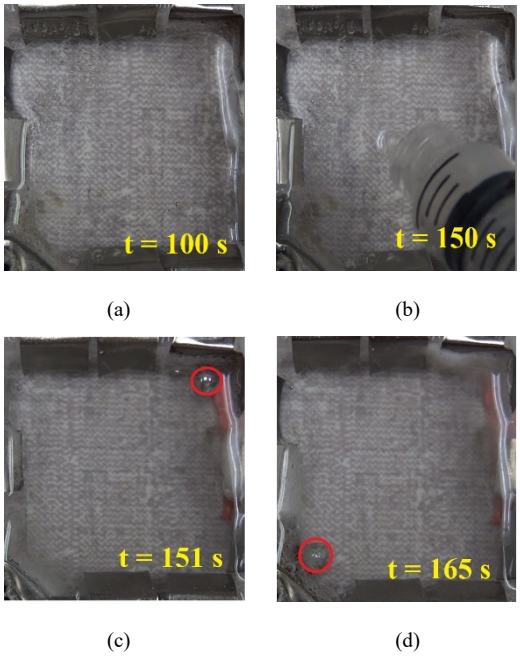

Fig. 6. Demonstration of hot-spot cooling. (a) NaOH well when voltage has beeen applied for 100 s. During this time period, the hot spot is generated in the NaOH near the top-right electrode by Joule heating. The total duration of activation of the top-right electrode is 165 s. (b) At the 150-s mark, the liquid-metal droplet is injected at the center of the NaOH well using a syringe (visible in this photo). The liquid-metal droplet moves toward the top-right by CEW, and reaches the hot spot within 1 s. (c) At the 151-s mark, the droplet is at the hot spot. The droplet remains in this location for ~ 10 s, then (d) the polarity of the signal is switched so that the droplet moves via CEW toward the bottom-left electrode, which serves as the heatsink. The droplet reaches the heat sink within 1 s. Once the droplet reaches the heat sink, it remains in contact with the heat sink until the experiment is terminated at 170 s. The location of the liquid-metal droplet is outlined in red in the photos.

A FLIR SC6xx series infrared camera mounted on a tripod recorded the heat map of the device. The *ResearchIR* software, compatible with the camera, is used to extract temperature data

from the recorded video. The temperature data was also measured and verified using an OMEGA thermometer with an OMEGA Type K thermocouple.

The heating caused by the activation of the top-right electrode was distributed throughout the region of interest (a 1 cm × 1 cm area in the top-right corner of the PDMS well) by the NaOH [Fig. 7(a)]. The applied voltage causes the temperature of the NaOH to slowly increase [Fig. 7(b)] at a rate of 0.39 °C/s for a 10-V signal, and 0.58 °C/s for an 11-V signal. The inset of Fig. 7(b) shows that the temperature increase is less than 0.5 °C over the duration of a typical CEW actuation signal.

C. *Hot-Spot Creation and Cooling*

As a baseline for investigating the effectiveness of liquid-metal-droplet hot-spot cooling, the process described in Fig. 6 was conducted without a liquid-metal droplet. In the absence of injecting a liquid-metal droplet into the device well, the Joule heating of NaOH continues to increase beyond the 150-s mark of electrode activation. Temperature measurements are taken for three time points with and without the liquid-metal droplet: before the voltage was applied ($t = 0$ s), after the voltage has been applied for 150 s, and after the voltage has been applied for 160 s (Fig. 8). The experiment was carried out for applied voltages of 10 V and 11 V.

Compared to the heat map for Joule heating at 10 V [Fig. 8(a)], there is a significant distribution of heat throughout the NaOH well at an applied voltage of 11 V [Fig. 8(b)]. The heat maps verify the results in Fig. 7(b), in which the NaOH temperature increases at a faster rate for higher voltage.

The liquid-metal droplet is manually injected at the 150-s mark. After approximately 10 s of the droplet occupying the hot spot ($t = 160$ s), a decrease in temperature of approximately 3 °C was achieved at the hot spot for an actuation voltage of 10 V [Fig. 8(c)]. For an actuation voltage of 11 V, a decrease in temperature of approximately 3 °C was observed at $t = 160$ s [Fig. 8(d)]. The cooling effect of the liquid-metal droplet at the hot spot competes with the continued Joule heating of the NaOH.

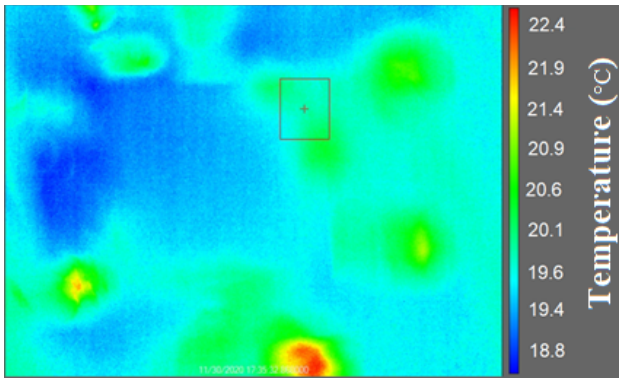

(a)

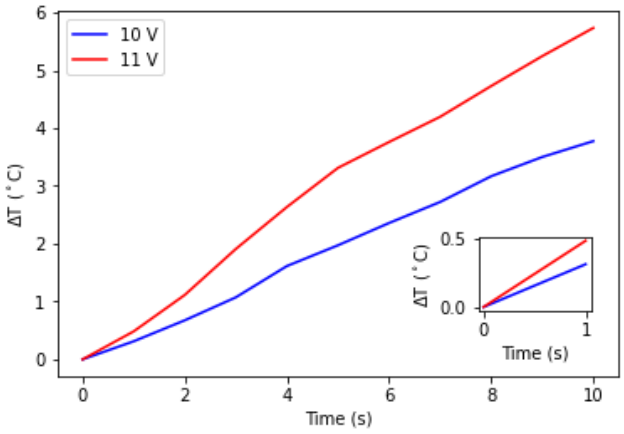

(b)

Fig. 7. (a) A region of interest was specified to measure the temperature at a 1 cm × 1 cm square in the upper-right corner of the NaOH well. (b) A temporal plot of ΔT for the region of interest. The inset represents the actuation time window.

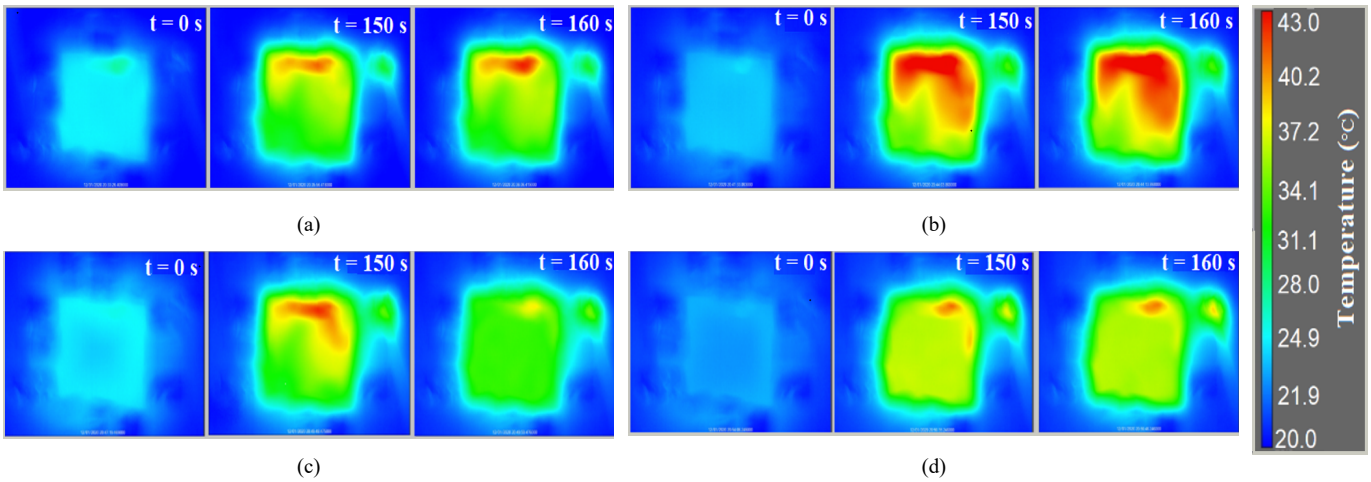

(a) (b) (c) (d)

Fig. 8. Time series of the device's heat map. The top row is without liquid metal at (a) 10 V and (b) 11 V. In the bottom row, a liquid-metal droplet is injected at 150 s with an actuation voltage of (c) 10 V and (d) 11 V.

The change in hot-spot temperature for the 10 V and 11 V actuation voltages is shown in Fig. 9. Each data point represents the average of four separate trials. At approximately t = 151 s there is a 7 °C temperature drop at the hot spot for an actuation voltage of 10 V. This suggests that the liquid metal is providing rapid cooling at the hot spot. A factor that can drastically affect the decrease in temperature is the heating rate of the electrodes and its interaction with the liquid-metal droplet. Since the change in voltage results in different slopes for the ΔT curves, some further investigation is necessary with the cooling rates of the droplet versus the heating rate of the hot spot.

Fig. 10 shows the temperature data averaged over the entire 3 cm × 3 cm NaOH well [Fig. 8(c) and Fig. 8(d)], instead of just the hot spot. Each data point represents the average of four separate trials. As the hot spot continues to increase in temperature, the entire well increases in temperature. As in Fig. 9, the temperature of the well decreases past the 150-s mark due to the liquid-metal droplet cooling the hot-spot region.

D. Effects of NaOH Electrolyte on Joule Heating

A further investigation with Joule heating was performed by adjusting the NaOH molarity. By varying the molarity of the NaOH solution within the well, the NaOH conductivity can be controlled. In Fig. 11, the change in temperature at the hot spot was measured for 1-M, 0.5-M, and 0.1-M NaOH. As the NaOH molarity increases, the NaOH conductivity should increase too. As shown in Fig. 11, the result was expected because a higher electrical conductivity results in a higher thermal conductivity.

Since NaOH molarity affects the flow of electrical current from the electrodes through the NaOH and thus affects heat, several conclusions can be drawn for future device construction. Since any NaOH molarity is sufficient to perform CEW actuation of liquid metals, decreasing the NaOH molarity helps the device retain less heat from actuation, or when holding the liquid-metal droplet at a particular location. The drawback of using a lower NaOH molarity, which is closer to a pure water solution, is that higher CEW actuation voltages are needed [13].

IV. Conclusion

Rapid hot-spot cooling using a liquid-metal droplet electrically actuated along an arbitrarily prescribed two-dimensional path has been demonstrated for the first time. For an actuation voltage of 10 V DC, the liquid-metal droplet decreases the temperature of a localized hot spot by approximately 7 °C. Liquid-metal droplet actuation along straight-line and arbitrary paths within a two-dimensional plane have been demonstrated. Thermal effects of applied actuation voltages and variations in NaOH molarity have been quantified.

Further improvements of this work, such as hot-spot temperature reductions greater than 7 °C or decreasing the size of the device, will improve its potential for use in chip-cooling applications.

Acknowledgment

This work was supported in part by the National Science Foundation under Grant ECCS 1807896.

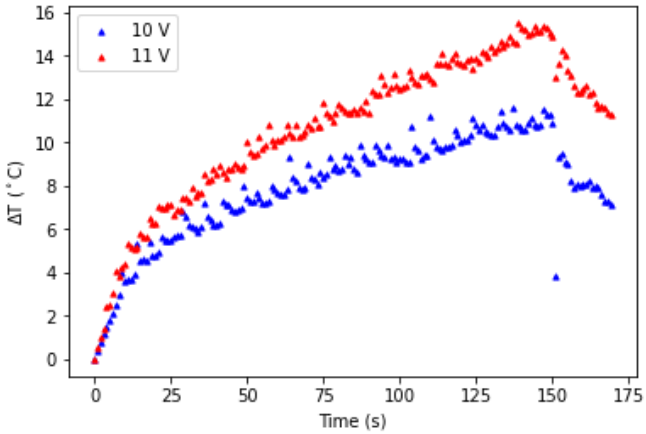

Fig. 9. Temporal plot of ΔT for the device's hot spot. The liquid-metal droplet is injected into the well at the 150-s mark, rapidly cooling the hot spot in a short time frame. The cooling rate of the droplet can be determined if there was a larger sampling resolution after the 150-s mark. After the sudden temperature decrease, the hot-spot temperature transitions to a higher temperature because the droplet moves away from the hot spot and toward the heat sink.

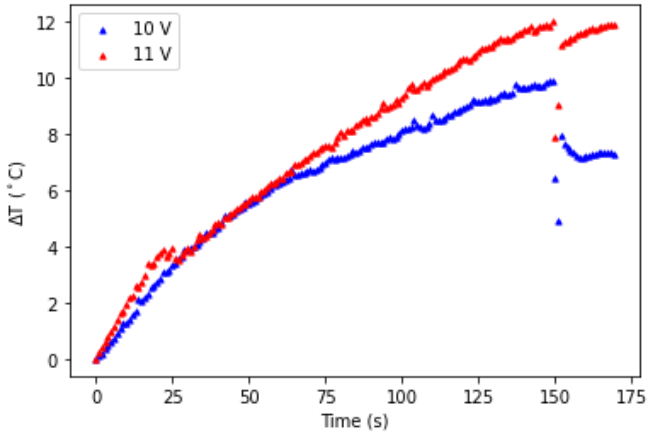

Fig. 10. Temporal plot of ΔT for the NaOH well with the liquid-metal droplet injected at the 150-s mark.

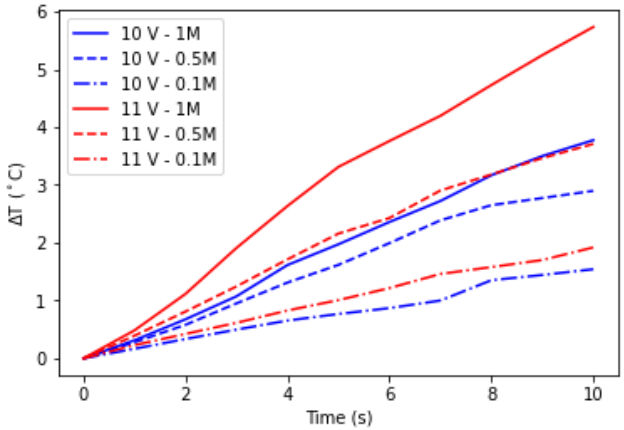

Fig. 11. A temporal plot of ΔT for various NaOH molarities . The 1-M (solid), 0.5-M (dashed), and 0.1-M (dash-dotted) NaOH have varying rates of temperature change.

REFERENCES

[1] K. Peng, J. Yao, S. Cho, Y. Cho, H. S. Kim, and J. Park, "Liquid metal embedded real time microfluidic flow pressure monitoring sensor," *Sensors and Actuators A: Physical*, vol. 305, p. 111909, 2020.

[2] J. So and M. D. Dickey, "Inherently aligned microfluidic electrodes composed of liquid metal," *The Royal Society Chemistry*, vol. 11, no. 5, pp. 905–911, 2011.

[3] R. Zhao, R. Guo, X. Xu, and J. Liu, "A fast and cost-effective transfer printing of liquid metal inks for three-dimensional wiring in flexible electronics," *ACS Applied Materials and Interfaces*, vol. 12, no. 32, pp.36723–36730, 2020.

[4] K. S. Elassy, M. A. Rahman, W. A. Shiroma, and A. T. Ohta, "Liquid-metal nodal sheet for reconfigurable devices and circuits," *IEEE Access*, vol. 8, pp. 167596–167603, 2020.

[5] C. B. Eaker and M. D. Dickey, "Liquid metal actuation by electrical control of interfacial tension," *Applied Physics Reviews*, vol. 3, no. 3, p. 031103, 2016.

[6] S. Tang, V. Sivan, P. Petersen, W. Zhang, P. D. Morrison, K. Kalantar-zadeh, A. Mitchell, and K. Khoshmanesh, "Liquid metal actuator for inducing chaotic advection," *Advanced Functional Materials*, vol. 24, no. 37, pp.5851–5858.

[7] X. Li, S. Li, Y. Lu, M. Liu, F. Li, H. Yang, S. Tang, S. Zhang, W. Li, and L. Sun, "Programmable digital liquid metal droplets in reconfigurable magnetic fields," *ACS Applied Materials and Interfaces*, vol. 12, no. 33, pp. 37670–37679, 2020.

[8] Z. Yan, M. Jin, Z. Li, G. Zhou, and L. Shui, "Droplet-based microfluidic thermal management methods for high performance electronic devices," *Micromachines*, vol. 10, no. 2:89, 2019.

[9] J. Lee and C. J. Kim, "Surface-tension-driven microactuation based on continuous electrowetting," *J. Microelectromech. Syst.*, vol. 9, no. 2, pp. 171–180, 2000.

[10] R. C. Gough, A. M. Morishita, J. H. Dang, W. Hu, W. A. Shiroma, and A. T. Ohta, "Continuous electrowetting of non-toxic liquid metal for RF applications," *IEEE Access*, vol. 2, pp. 874–882, 2014.

[11] J. Y. Zhu, S. Tang, K. Khoshmanesh, and K. Ghorbani, "An integrated liquid cooling system based on Galinstan liquid metal droplets," *ACS Applied Materials and Interfaces*, vol. 8, no. 3, pp. 2173–2180, 2015.

[12] D. Brown, R. Hanson, and W. Christian, *Tracker Video Analysis and Modeling Tool for Physics Education*. [Online]. Avaialble: https://physlets.org/tracker/. [Accessed: 14-Dec-2020].

[13] L. Sheng, J. Zhang, and J. Liu, "Diverse transformation of liquid metals between different morphologies," *Advanced Materials*, vol. 26, pp. 6036–6042, 2014.

.